

Reversal of the Fluctuation-Induced Transport during Low to High Transitions in the H-1 Helic Plasma

M. G. Shats and D. L. Rudakov

*Plasma Research Laboratory, Research School of Physical Sciences and Engineering,
Australian National University, Canberra, ACT 0200, Australia*

(Received 21 March 1997; revised manuscript received 5 August 1997)

Studies of turbulent transport in the H-1 heliac plasmas yield direct evidence of the reversal of the fluctuation-driven particle flux across the transition from low to high confinement mode. New types of transitions are characterized by significant fluctuation levels in the high confinement mode. The fluctuation-driven particle flux in the plasma core changes from outward to inward flow across this transition; this is accompanied by a peaking of the density profile and an increase in central ion temperature. [S0031-9007(97)04142-2]

PACS numbers: 52.55.Hc, 52.25.Fi, 52.25.Gj

Studies of the fluctuation-induced transport in magnetically confined plasmas have long been important in fusion research. This problem has become a focus of experimental and theoretical work with regard to sudden transitions to improved confinement modes, such as the low-to-high transitions in tokamaks and stellarators. In general, it is expected that high fluctuation amplitudes lead to unfavorable outward transport of particles and energy.

In this Letter we present direct evidence of a reversal in the radial fluctuation-induced particle flux during a low-to-high confinement transition in the H-1 stellarator, the first such observation in a toroidally confined plasma.

Depending on the experimental conditions, the transition can be to either “quiescent” or “fluctuating” high mode. During the transition to the quiescent high mode, the fluctuations subside, and outward-directed fluctuation-induced particle flux is reduced by almost 2 orders of magnitude. However, during the transition to the fluctuating high mode, the fluctuations persist, but the fluctuation-induced particle flux reverses direction.

The H-1 stellarator is a flexible heliac configuration [1,2] and, for the experiments reported here, was operated in a shearless magnetic configuration with $\iota \approx 1.45$, $B = 0.05\text{--}0.15$ T, and a radio frequency heating power of up to 100 kW at the frequency of 7 MHz. Central electron density is about 10^{18} m^{-3} , the electron temperature in argon discharges is in the range from 8 to 20 eV, and the ion temperature is about 40–50 eV in the low confinement mode.

The transition to the quiescent high confinement mode has been reported in Refs. [3,4]. In that case, the transition is correlated with a significant increase in the electron density, ion temperature, and radial electric field and is accompanied by a reduction in Γ_{fl} by ~ 2 orders of magnitude. A time history of the average electron density is shown in Fig. 1(a). The density increases in <1 ms to a new steady state with $\sim 10\times$ smaller density (\bar{n}_e) fluctuations and plasma potential ($\tilde{\phi}_{pl}$) fluctuations [3]. These fluctuations are global drift modes [5] having low poloidal m and toroidal n mode numbers ($m = 1, 2$) and frequen-

cies in the range of 4–15 kHz in argon discharges. The transitions are not accompanied by the changes in the bulk plasma rotation whose velocity (both poloidal and toroidal components) is small compared with the $\mathbf{E} \times \mathbf{B}$ drift velocity [4].

Such transitions are observed at a filling pressure of the working gas p_{gas} (argon in the present experiments) above 3×10^{-5} torr. At lower pressures of about $p_{gas} = (1 - 2) \times 10^{-5}$ torr, spontaneous transitions to improved confinement are observed at about 20% lower magnetic fields. In these conditions the improved confinement mode is characterized by up to a 70% increase in the average electron density, up to a 100% increase in the ion temperature

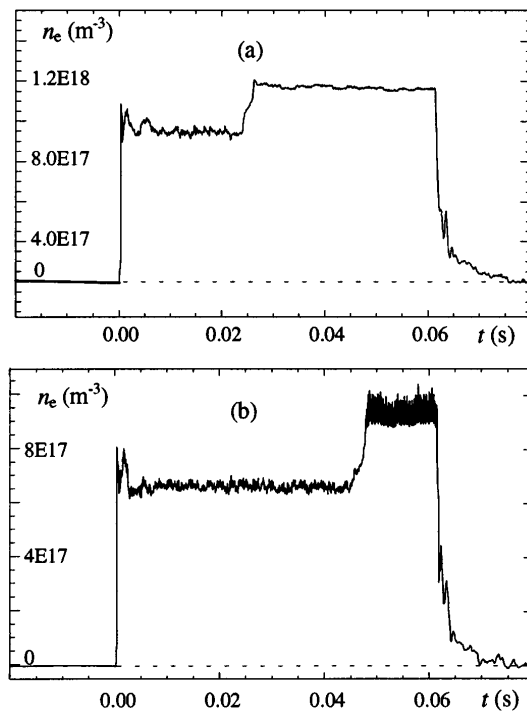


FIG. 1. Time history of the average electron density during the transitions to the quiescent (a) and fluctuating (b) high confinement modes.

(from 50 eV to about 100 eV), and more peaked n_e and T_i profiles similar to those in the quiescent high mode [4]. The major difference between the two modes of improved confinement is that the fluctuation level does not show any significant decrease across the transition to the fluctuating high mode. In some cases the fluctuation level even increases in high mode, as shown in Fig. 1(b).

A retarding field energy analyzer [4] is used to measure the ion temperature and the plasma potential. A modified version of a triple probe [6] is used to measure the ion saturation current I_s , the electron temperature, the plasma potential φ_{p1} , and the poloidal wave numbers k_{pol} of the fluctuations. The probe assembly consists of the two triple probes separated poloidally by 15 mm. This “double-triple” probe is then used to compute the poloidal wave numbers of the fluctuations.

Figure 2 shows the frequency spectra of the fluctuations of the ion saturation current [Figs. 2(a) and 2(c)] and the fluctuation-induced particle flux Γ_{fl} [Figs. 2(b) and 2(d)] before and after the transition to the fluctuating high mode. Γ_{fl} is computed as

$$\Gamma_{fl}(\omega) = \frac{k_{pol}(\omega)}{B} \tilde{n}_e(\omega) \tilde{\varphi}_{p1}(\omega) \gamma(\omega) \sin \theta(\omega), \quad (1)$$

where the electron density fluctuations \tilde{n}_e are obtained from the fluctuations of the ion saturation current \tilde{I}_s and the electron temperature \tilde{T}_e (since $I_s \sim n_e \sqrt{T_e}$), plasma potential fluctuations $\tilde{\varphi}_{p1}$ are estimated as $\tilde{\varphi}_{p1} = \tilde{\varphi}_f + 3.8\tilde{T}_e$ ($\tilde{\varphi}_f$ is the floating potential fluctuations), k_{pol} is the poloidal wave number defined during the same time interval from the phase shift between two poloidally separated probes, and γ and θ are, correspondingly, the coherence and phase shift between the fluctuations of the electron density and the plasma potential. Negative values of Γ_{fl} correspond to outwardly directed particle flux. After the transition [Fig. 2(d)], the sign of Γ_{fl} changes to positive, indicating inwardly directed flux. The change in the flux

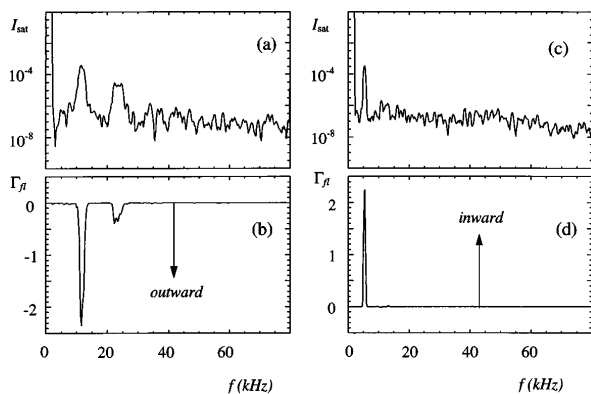


FIG. 2. Frequency spectra of the fluctuations of the ion saturation current [(a) and (c)] and fluctuation-induced particle flux Γ_{fl} [(b) and (d)] at $r/a = 0.44$ before and after the transition to the fluctuating high mode of Fig. 1(b).

direction is due principally to a change in the phase shift between \tilde{n}_e and $\tilde{\varphi}_{p1}$. Sensitivity tests show that our conclusions are not sensitive to details of our probe model, e.g., the value of the coefficient of T_e in the expression for φ_{p1} . The level of the background broadband turbulence sometimes increases after the transition with respect to the amplitude of spectral peaks, but its contribution to the net flux Γ_{fl} remains small (less than 2%) compared with the contribution of the strongest frequency harmonics.

The transition to improved confinement leads to the significant increase in the electron density on a major part of the plasma radius, as shown in Fig. 3(a), and to the reversal of the fluctuation-induced particle transport shown in Fig. 3(b). This effect is observed both inside and outside the magnetic axis (dashed line in Fig. 3). The experimental geometry is illustrated in Fig. 4(a), where the solid line across the flux surfaces shows the probe scanning chord. The profiles in Fig. 3 were obtained on a shot-to-shot basis, but only shots with identical spontaneous transitions from low to high confinement are used. To monitor the perturbation of the plasma caused by the scanning double-triple probe, we used another triple probe

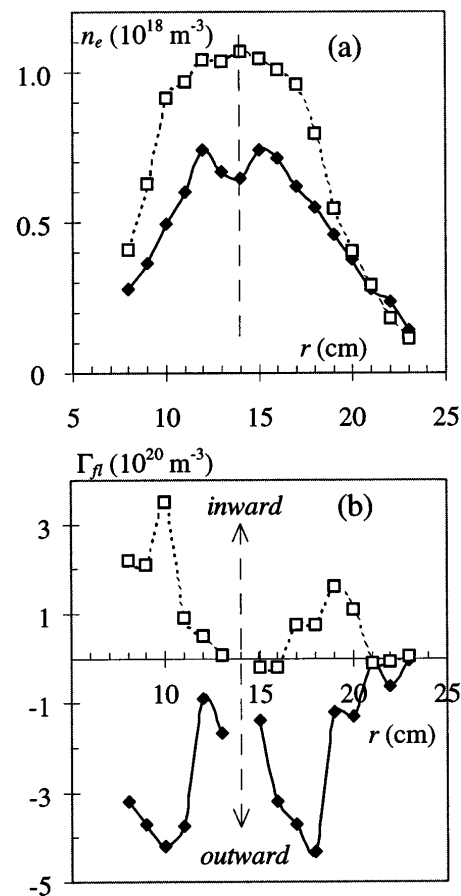


FIG. 3. Radial profiles of the electron density (a) and the fluctuation-induced particle flux (b) before (diamonds) and after (squares) the transition from low to the fluctuating high confinement mode.

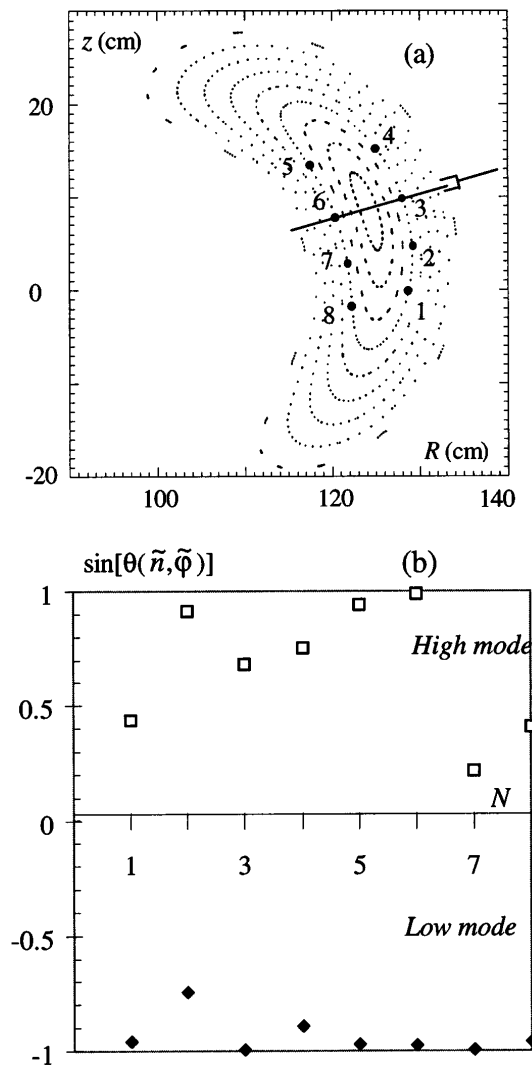


FIG. 4. Flux surfaces and the probe scanning chord (solid line) in the plasma poloidal cross section (a); sine of the phase between density and potential fluctuations versus the number of points on a flux surface (b).

separated toroidally by about 15 cm from the scanning probe and located at the same flux surface. Again, only shots with similar transitions seen by the monitoring probe were used.

It has been experimentally observed [7] that the fluctuation-induced flux can be nonuniform on the magnetic surface. We have confirmed the effect of the Γ_{fl} reversal at several points on the same flux surface. The location of the points on the flux surface is shown in Fig. 4(a). Figure 4(b) shows a sine of the phase shift between \tilde{n}_e and $\tilde{\varphi}_{p1}$ versus a point number on a flux surface ($r/a \approx 0.5$). This phase shift [see Eq. (1)] reverses after the transition for all the points shown in Fig. 4, suggesting thus that the effect of the flux reversal is uniform on a flux surface.

Comparison of the flux profiles for various detailed scenarios of low-to-fluctuating high transitions (variation of rf

power, filling pressure) show essentially similar behavior to that in Fig. 3. The net improvement in the particle confinement seen on the average density [Fig. 1(b)] and the density profiles [Fig. 3(a)] during the transition correlates with the observed Γ_{fl} modification.

The modifications in the fluctuation-induced transport during the transitions to improved confinement modes have been discussed from both experimental and theoretical standpoints [8,9]. Some recent experimental observations (e.g., Ref. [10]) indicate that it is the decorrelation of the density and potential fluctuations rather than just the reduction of the fluctuation amplitude that affects Γ_{fl} . In our experiment both the magnitude and direction of Γ_{fl} change due to the “recorelation” (change of relative phase) of \tilde{n}_e and $\tilde{\varphi}_{p1}$.

In Ref. [11] it was shown that the local fluctuation-induced fluxes in L-mode discharges have an intermittent character. In H-1, we find this to be the case in both low and high confinement modes. The time-resolved flux $\Gamma_{fl}(t) = \tilde{n} \tilde{E}_{pol} / B$, normalized to its mean value [$\Gamma_n = \Gamma_{fl}(t) / \langle \Gamma_{fl}(t) \rangle$] is shown in Fig. 5 for both low mode and high mode. The positive and negative spikes in $\Gamma_{fl}(t)$ characterize inward and outward “transport events” [11]. The effect of the reversal of the average flux across the transition can be seen clearly in Fig. 5. Despite the quasicohherent nature of the fluctuations in H-1 (seen in the frequency spectra of Fig. 2), the local fluxes are intermittent in both confinement modes.

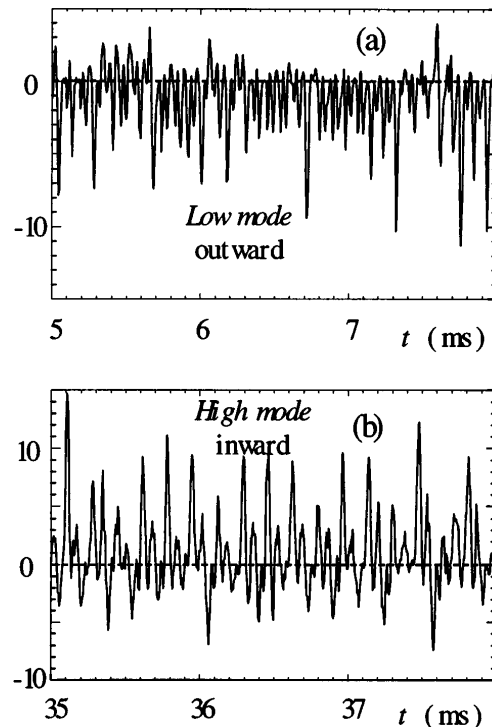


FIG. 5. Time evolution of the time-resolved local fluctuation-induced flux $\Gamma_n = \Gamma_{fl}(t) / \langle \Gamma_{fl}(t) \rangle$ at $r/a = 0.5$ before (a) and after (b) the transition to the improved confinement mode.

The net particle flux includes both the background and the fluctuation-induced diffusivities:

$$\Gamma_{\text{total}} = D \frac{dn}{dr} + \Gamma_{\text{fl}}.$$

To estimate the relative contribution of Γ_{fl} to the net flux and its role in the particle confinement in H-1, we analyze the particle balance. First, we estimate the $D(dn/dr)$ component of the flux from the ionization balance based on the experimental data on the neutral density distribution in the plasma. The neutral density is derived from the measured radial profiles of the spectral line intensities of excited neutrals and ions, and the electron density and electron temperature profiles measured using triple probes [4]. Since the recombination rate is negligibly small in our conditions (2 to 3 orders of magnitude lower than the ionization rate), the ionization is balanced by the outward transport. The net particle flux at $r/a = 0.9$ calculated for the conditions of the quiescent high confinement mode is about $\Gamma_{\text{total}} \approx 3 \times 10^{20} \text{ m}^{-2} \text{ s}^{-1}$. Since in the quiescent high mode the contribution of the fluctuations to the particle transport is very small [3], we obtain $D \sim 25 \text{ m}^2 \text{ s}^{-1}$ from this estimate.

Second, we estimate the outward radial ion flux from measurements using a radially oriented Mach probe at the plasma periphery. From the in-out asymmetry of the radial ion flows to the probe (the ion saturation current asymmetry factor is about 2), we estimate the net outward ion flux to be $\Gamma_{\text{total}}(r/a = 0.9) \approx 4 \times 10^{20} \text{ m}^{-2} \text{ s}^{-1}$ which is very close to the above estimate obtained from the ionization balance. In the inner region of plasma, at $r/a = 0.6$, similar analysis gives $\Gamma_{\text{total}}(r/a = 0.6) \approx 2 \times 10^{20} \text{ m}^{-2} \text{ s}^{-1}$ which is of the order of magnitude of the fluctuation-induced component of the flux in the

fluctuating high mode $\Gamma_{\text{fl}} \approx 3 \times 10^{20} \text{ m}^{-2} \text{ s}^{-1}$ shown in Fig. 3(b).

The correlation of the reversal of the fluctuation-driven component of the particle flux and the improvement in the particle confinement suggest a casual relationship.

In summary, we have measured fluctuation-induced particle flux in H-1 stellarator discharges that spontaneously pass through a low-to-high confinement transition. This flux exhibits an intermittent character in both the low and high modes, and reverses direction to flow radially inward in the plasma core in the high mode. The reversal results from the change in the relative phase of density and potential fluctuations. While these experiments in H-1 were done at low plasma temperatures and densities, the results suggest a paradigm that may be applicable to other experiments.

The authors would like to thank J.H. Harris, G.G. Borg, B.D. Blackwell, and N.N. Skvortsova for many useful discussions of the results; R. Davies, G. McCluskey, J. Wach, and T. McGuinness for the operational support; and R. Kimlin for the help in fabricating the probes.

-
- [1] J.H. Harris *et al.*, Nucl. Fusion **25**, 623 (1985).
 - [2] S.M. Hamberger *et al.*, Fusion Technol. **17**, 123 (1990).
 - [3] M.G. Shats *et al.*, Phys. Rev. Lett. **77**, 4190 (1996).
 - [4] M.G. Shats *et al.*, Phys. Plasmas (to be published).
 - [5] M.G. Shats *et al.*, Trans. Fusion Technol. **27**, 286 (1995).
 - [6] S. Chen and T. Sekiguchi, J. Appl. Phys. **36**, 2363 (1965).
 - [7] P.G. Matthews *et al.*, Phys. Fluids B **5**, 4061 (1993).
 - [8] R.A. Moyer *et al.*, Phys. Plasmas **2**, 2397 (1995).
 - [9] D.E. Newman *et al.*, Phys. Plasmas **3**, 1858 (1996).
 - [10] G.R. Tynan *et al.*, Plasma Phys. Control. Fusion **36**, A285 (1994).
 - [11] B.A. Carreras *et al.*, Phys. Plasmas **3**, 2664 (1996).